Statistical mechanics of axisymmetric vortex rings

R. Ganesh* and K. Avinash
Institute for Plasma Research, Bhat, Gandhinagar 382 428, India
(Received 23 October 2000; revised manuscript received 4 October 2001; published 14 January 2002)

We construct maximum entropy states of a collection of interacting uniform ($\omega/R=$const) axisymmetric vortex rings in a semiperiodic bounded volume. Following Miller [Phys. Rev. Lett. **65**, 2137 (1990)] and Robert and Sommeria [J. Fluid Mech. **229**, 291 (1991)], we obtain an equilibrium measure that preserves all the ideal invariants such as the total energy, total impulse, circulation, and an infinity of Casimirs. The numerical solution for a wide range of total flow energy and for given values of total circulation and total impulse is presented.

DOI: 10.1103/PhysRevE.65.026402 PACS number(s): 47.32.Cc, 47.27.Jv

I. INTRODUCTION

The formation of coherent vortical structures in two-dimensional (2D) hydrodynamic turbulence has attracted much attention [1]. In the past, many interesting statistical mechanical models have been proposed to address this issue. For example, Onsager [2] introduced the concept of *negative temperature* in his point (or line) vortex model, wherein a continuous 2D vorticity field is decomposed into large number of point (or line) vortices interacting with each other through a logarithmic potential. Later, Taylor [3] first obtained an expression (though incorrect) for W_c, the critical energy for transition from positive to negative temperatures for a neutral vortex gas. Montgomery and Joyce [4] corrected Taylor's expression by subtracting the self-energy component of individual point vortices; they also constructed a mean field theory for such a collection of N-point vortices using Boltzmann's combinatorial method. Edwards and Taylor [5] obtained the equation of state; and Seyler [6] gave the quantitatively correct expression for W_c by including the effect of *image* vorticity. Pointin and Lundgren [7] constructed the nonlinear partial differential equations for neutral and non-neutral point vortex systems; they also gave a rigorous proof of the equation of state with an arbitrary boundary shape using the Kirchhoff-Routh technique. For a more comprehensive discussion of the statistical mechanics of point vortices we refer the reader to Ref. [8] and references therein. For an alternative viewpoint regarding the definition of temperature for a finite dimensional vortex system, etc., see Ref. [9] and references therein.

More recently, Miller *et al.* [10] and Robert and Sommeria [11] (MR) proposed a statistical mechanical theory that qualitatively reproduces many numerically observed features of coherent structure formation in planar Euler flows [12,13]. Miller constructed a family of discrete vorticity fields that could share common values for a large number of Casimirs (invariants) by simply permuting the vorticities in a finite number of boxes (the group of area-preserving diffeomorphisms). The free energy of this many-invariant system is obtained by assuming a scale separation between *microscopic* and *macroscopic* vorticity fluctuations which with the long range of the Coulomb interaction leads to an exact mean field theory. On the other hand, Robert and Sommeria obtained the same mean field equations, which respect the invariance of the Casimirs, by introducing a Boltzmann-Shannon-Jaynes information-theoretic entropy functional. In contrast to the permutative methods (such as Miller's) which crucially depend on the strong assumption of ergodicity, Robert and Sommeria prove a weak concentration property of the underlying microstates (flow) that allows them to define a macrostate probability distribution, which is shown to be "the most probable probability distribution function" among all possible distributions subject to the information already known (i.e., invariance of energy and Casimirs).

Another such interesting class of hydrodynamic flows are the *axisymmetric* flows in inviscid, incompressible fluids; in such flows, the equivalent of a line vortex is a vortex ring. Unlike their planar counterparts, vortex rings have self-induced motion (because one part of a vortex ring can interact with another part of itself); consequently, an individual vortex ring embedded in a fluid has many interesting features. In the past, there has been a large body of work on such "deterministic" (as against our "turbulent") steady, axisymmetric vortex rings. For example, Maruhn [14] and Fraenkel [15] showed theoretically the existence of vortex rings with small cross sections. Norbury [16,17] obtained numerically the self-induced uniform speed, the shape of the cross section, and the stream function of a uniform vortex ring. Similar studies have been reported on hollow or stagnant vortex rings [18] and convex vortex rings [19], etc. In particular, the uniform axisymmetric vortex ring has been a favorite for over a century; the best known example is Hill's spherical vortex, which is the only steady "ring" (of zero radius) represented by an exact solution in closed form. Wan [20] applied a variational technique for a single fat ring embedded in an infinite fluid; he obtained Hill's vortex as a "nondegenerate" maximum of energy subject to a fixed value of impulse and Norbury's spherical vortex ring with a hole as an extremum state of energy subject to fixed values of both impulse and circulation.

The stability aspects of vortex rings have also attracted considerable attention. Notably, Widnall and co-workers [21,22] have shown that vortex rings are unstable along the

*Present address: Department of Electrical Engineering, Pohang University of Science and Technology (POSTECH), Pohang, S. Korea. Electronic address: ganu@kitty.postech.ac.kr

perimeter even according to ideal flow theory. More recently, there has been a lot of interest in the formation of vortex rings [23], in the so-called universal "formation time" of nearly inviscid axisymmetric vortex rings [24], etc. However, although considerable attention has been paid to the properties of a single deterministic vortex ring, very few reports (almost none) exist so far on a statistical equilibrium theory of formation of (in general) nonuniform, steady vortex rings as coherent structures (macrostates) arising out of turbulent conditions.

In the present work, we propose one such statistical mechanical theory for axisymmetric Euler flows, along the lines of MR statistics, for construction of late time turbulent coherent structures. In particular, we will restrict ourselves to a collection of axisymmetric vortex rings in a semiperiodic, bounded domain and construct axisymmetric maximum entropy states out of interacting uniform vortex rings ($\omega/R = \text{const}$) of small but finite core size ("hard core"). Late time structures thus constructed are shown to be macroscopically uniform or nonuniform, depending upon the initial values of "robust" conserved quantities such as total energy, impulse, and circulation. Our formulation also conserves an infinite number of Casimirs (integrals of arbitrary but sufficiently smooth functions of ω/R) and other constants arising out of the symmetry of the confining geometry. The theory is elucidated by numerically solving the mean field equations for a simple initial condition with two-level vorticity.

In Sec. II, we present the geometry, the model equations, and the conservation laws. In Sec. III, the statistical mechanical formulation is presented, which results in a set of mean field equations. In Sec. IV we present numerical solutions of the mean field equations for the special case of initial conditions with two vorticity levels. In Sec. V we discuss the validity of our model and other open questions relevant to both planar and axisymmetric Euler flows.

II. MODEL EQUATIONS

We use cylindrical coordinates to describe the dynamics of axisymmetric Euler flows in a domain V (see Fig. 1). Our basic equation is the well known vorticity equation [25] of an axisymmetric, inviscid, incompressible flow given by

$$\frac{\mathcal{D}\omega}{\mathcal{D}t} = (\boldsymbol{\omega}\cdot\boldsymbol{\nabla})\mathbf{v} \quad \text{with} \quad \boldsymbol{\omega} = \boldsymbol{\nabla}\times\mathbf{v} \tag{1}$$

where $\mathcal{D}/\mathcal{D}t = \partial/\partial t + (\mathbf{v}\cdot\boldsymbol{\nabla})$.

In Cartesian three-space, if the flow is planar then the right hand side (which is also called the *stretching term*) of Eq. (1) is identically zero. In an axisymmetric flow without swirl (i.e., axisymmetric component of the flow) since $\mathbf{v} = [v_R, 0, v_Z]$ the flow is only in the (R,Z) plane. Consequently, the vorticity equation will have only the θ component, i.e., $\boldsymbol{\omega} = [0, \omega_\theta, 0]$ (which henceforth will be referred to as ω), whose governing equation is given by

$$\frac{\partial\omega}{\partial t} + v_R\frac{\partial\omega}{\partial R} + v_Z\frac{\partial\omega}{\partial Z} = \frac{\omega v_R}{R}.$$

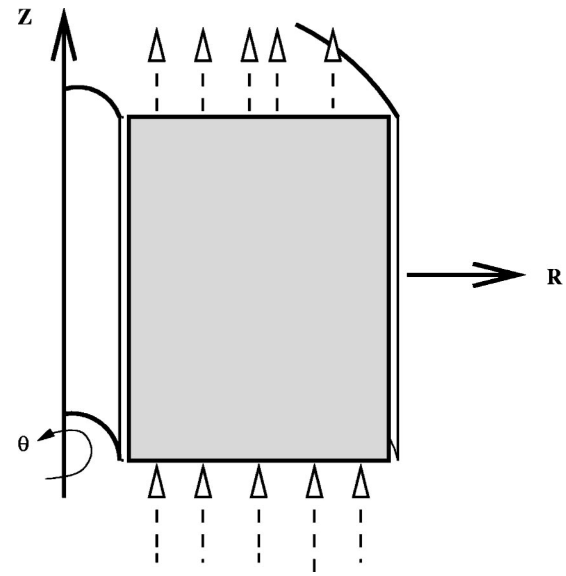

FIG. 1. Schematic view of the coordinate system; the **Z** direction is periodic, the **R** direction is bounded.

This can be rewritten as

$$\frac{\mathcal{D}\Omega}{\mathcal{D}t} = 0 \tag{2}$$

where $\Omega = \omega/R$ is the vorticity per unit length. For convenience, we refer to Ω as the vorticity throughout. Equation (2) can be classically solved by introducing the stream function for axisymmetric flow Ψ such that

$$\mathbf{v} = \boldsymbol{\nabla}\times\left(\frac{\Psi}{R}\hat{\boldsymbol{\theta}}\right) \tag{3}$$

and ω can be rewritten as

$$-\Delta^*\Psi = -\left(\frac{\partial^2}{\partial R^2} + \frac{\partial^2}{\partial Z^2} - \frac{1}{R}\frac{\partial}{\partial R}\right)\Psi = R^2\Omega, \tag{4}$$

where Δ^* is the operator indicated in the parentheses. The value of the associated stream function Ψ can be specified at the boundaries, which in turn [through Eq. (3)] will determine the flow pattern at the boundaries.

Equation (2) conserves the total flow energy W, impulse P, total circulation C, and an infinity of Casimirs, say I_f (defined below), arising out of conservation of Ω along the flow. The total flow energy is given by [25]

$$W = \pi\int_V \Psi\,\omega\, dR\, dZ = \frac{1}{2}\int_V \Psi\,\Omega\, d\mathbf{x} \tag{5}$$

where $d\mathbf{x} = 2\pi R\, dR\, dZ$ and V is the volume bounded by the boundary ∂V (for convenience, the value of fluid density ϱ, which is a constant, is set to unity).

If f is any smooth function of Ω, then the Casimirs I_f defined by

$$I_f = \int f(\omega) dR\, dZ = \int f(\Omega) d\mathbf{x} \tag{6}$$

are all conserved by the axisymmetric Euler flow. One can also see that the total circulation C is a member of I_f when $f(\Omega)=\Omega$, i.e.,

$$C = \int \Omega\, d\mathbf{x}. \tag{7}$$

The total fluid impulse P is defined as

$$P = \pi \int \omega(R^2 - R_0^2) dR\, dZ = \frac{1}{2} \int \Omega(R^2 - R_0^2) d\mathbf{x}. \tag{8}$$

Note that the above definition could be referred to as the *relative* impulse. It must be clear that the usual definition for the total impulse P_N (say) is related to P through circulation, i.e., $P_N = P + R_0^2 C/2$.

It should be obvious from the equations presented above that, although the integrals are defined over the volume element $d\mathbf{x}$, the definition is only formal. The entire formulation is relevant only in the incompressible plane (R,Z), making it effectively two dimensional.

III. STATISTICAL MECHANICAL FORMULATION

Euler flows are known to possess Hamiltonian structure [26,27]. However, the problem of finding canonically conjugate coordinates for such Hamiltonian flows has not yet been solved. Thus, in general, the existence of Liouville's theorem for systems governed by such noncanonical Hamiltonian flows is questionable. Nevertheless, a large class of systems that may be classified as noncanonical Hamiltonian flows are shown to be amenable to statistical mechanical treatment using what are known as Lie-Poisson brackets [28]. For example, in their elegant work Miller *et al.* [10] formulated the statistical mechanics of Euler flow using ideas developed in Ref. [28]. Here, however, we follow Robert and Sommeria [11].

A. Entropy

To define an appropriate phase space, note that the vorticity transport equation [Eq. (2)] is known to be well posed for bounded, measurable vorticity functions [29]. More precisely, if $\Omega^0(\mathbf{x}) = \Omega(\mathbf{x}, t=0)$ is a member of the ∞ function space of Ω's in the domain V, i.e., $\mathcal{L}^\infty(V)$, at some initial time $t=0$, then for all time $t>0$, $\Omega(\mathbf{x},t)$ will be a member of $\mathcal{L}^\infty(V)$ with $\sup|\Omega(\mathbf{x},t)| = \sup|\Omega^0(\mathbf{x})|$. From the transport equation shown above [Eq. (2)] it follows that *the maximum vorticity value at time $t=0$ is preserved by the flow dynamics during all times.* This bound provides sufficient smoothness on the velocity field [see Eq. (3)] to ensure the existence and uniqueness of fluid particle paths $\dot{\mathbf{x}} = \mathbf{v}(\mathbf{x},t)$, $\mathbf{x}(t=0)$. Thus, we consider an infinite collection of bounded vorticity functions $\Omega(\mathbf{x})$ that satisfy Eq. (2) as our phase space. With time, the solutions to Eq. (2) become rapidly irregular even when the initial vorticity function is smooth. This phenomenon is due to the growth of a vorticity gradient that results from the complex distortions suffered by the vorticity as it is advected in the flow it induces. To formulate a question at late times, these microstates $[\Omega(\mathbf{x})]$ would have to be connected to a macrostate through a proper entropy functional.

To define our macrostate, a number of assumptions regarding the nature of the flow are necessary to proceed further. We assume that the underlying flow is *ergodic*. Furthermore, without attempting to prove it, if some form of concentration property (similar to the one proved by Robert and Sommeria [11] for planar flows) of accumulation of a large number of microstates (consistent with the conserved quantities) in the neighborhood of a macrostate (defined below) is assumed, then the actual flow evolution will mostly stay near the macrostate.

We now proceed to show using heuristic combinatorial arguments how such a macrostate could be defined. For clarity of presentation, we focus on a simple case when the initial vorticity field $\Omega^0(\mathbf{x})$ is made up of n small patches of given vorticity levels $\{a_i\}$, $i=1,2,\ldots,n$, each level occupying a total "area" $\{A_i\}$. Due to the nature of the underlying flow, it is reasonable to expect vorticity fluctuations of all possible levels at any point $\mathbf{x}$ at $t=\infty$. Let $\{e_i(\mathbf{x})\}$ be the probability of finding levels $\{a_i\}$ at $\mathbf{x}$ at $t=\infty$. We would like to determine that particular field, say $\{e_i^*\}$, out of all possible probability fields consistent with the constants of motion, which would maximize a certain entropy functional. Thus $\{e_i\}$ will be our macrostate.

To obtain such an entropy functional, let us first consider a small region of area $\mathcal{A}$ around a point $\mathbf{x}$. At $t=\infty$, one may expect to find all possible vorticity levels $\{a_i\}$, each level occupying a small area $\{\mathcal{A}_i\}$. If the domain $\mathcal{A}$ is divided into N equal, nonintersecting subparts and if N_i is the number of such subparts having the vorticity level a_i, then $e_i(\mathbf{x}) = \mathcal{A}_i/\mathcal{A}|_x = N_i/N|_x$. The number of ways in which such a field $\{e_i(\mathbf{x})\}$, $i=1,\ldots n$, can be obtained by permuting the subparts is given by the weight $W(\{e_i(\mathbf{x})\}) = N!/(N_1!N_2!\cdots N_n!) = N!/[(e_1N)!(e_2N)!\cdots(e_nN)!]$. Here we have used Fermi counting for nonoverlapping subparts. Then the normalized logarithmic weight at $\mathbf{x}$ in the limit of infinite subparts, i.e., when $N\to\infty$, is given by $-\sum_{i=1}^n e_i(\mathbf{x}) \ln e_i(\mathbf{x})$. The limit $N\to\infty$ becomes necessary in order to define an entropy functional without introducing any artificial length scales (at which the vorticity fluctuations may be washed out). Upon computing for the entire domain V, the entropy of the macrostate $\{e_i(\mathbf{x})\}$ becomes

$$S(\{e_i(\mathbf{x})\}) = -\int_V \sum_i e_i(\mathbf{x}) \ln[e_i(x)] d\mathbf{x}. \tag{9}$$

It is important to note that for the microstates $[\Omega(\mathbf{x})]$ to be equiprobable, the flow should be necessarily mixing, i.e., ergodic. Once this condition is satisfied, the maximum entropy state is then the most probable state.

B. Constants of motion in terms of macrostates $\{e_i(\mathbf{x})\}$

The constants of motion restrict the macrostate by constraining the accessible microstates to a submanifold of the phase space. For an initial condition of nonoverlapping patches of vorticity a_i, the Casimirs $I_f = \int_V f(\Omega) d\mathbf{x}$ may be written as $\Sigma_i f(a_i) A_i$, which is simply the discrete sum of the continuum Casimir integral, where A_i is the *total* area containing the vorticity level a_i. Since the axisymmetric Euler flow preserves a_i and consequently $f(a_i)$, the conservation of Casimirs amounts to conservation of A_i for each i. Thus, in terms of the fractional area $e_i(\mathbf{x})$ at $\mathbf{x}$, the total area A_i becomes

$$A_i = \int_V e_i(\mathbf{x}) d\mathbf{x}. \tag{10}$$

Note that at each point $\mathbf{x}$ the total probability should add up to 1, i.e., $\Sigma_{i=1}^n e_i(\mathbf{x}) = 1$. To express other constants of motion in terms of the macrostate variables $e_i(\mathbf{x})$, we proceed as follows. Since the microscopic vorticity field $\Omega(\mathbf{x})$ at any point $\mathbf{x}$ is fluctuating rapidly, the macroscopic or measured vorticity at any point $\mathbf{x}$ will be the average of each vorticity level a_i according to its local probability $e_i(\mathbf{x})$ at that point. That is,

$$\overline{\Omega}(\mathbf{x}) = \sum_i a_i e_i(\mathbf{x}). \tag{11}$$

The constants of motion such as P, the total fluid impulse, that are linear functions of the microscopic fields $[\Omega(\mathbf{x})]$ can be written directly in terms of the probability field $e_i(\mathbf{x})$ and hence in terms of $\overline{\Omega}(\mathbf{x})$, as it is reasonable to replace the fluctuating microscopic field with its local average defined in Eq. (11). Thus, Eq. (8) becomes

$$P = \frac{1}{2} \int \overline{\Omega}(\mathbf{x})(R^2 - R_0^2) d\mathbf{x}. \tag{12}$$

The Green function is defined for our problem as [20]

$$-\frac{R_0^2}{R^2} \Delta^*_{R,Z} \mathcal{G}_\Psi = \delta(\mathbf{x} - \mathbf{x}'), \tag{13}$$

whose solution for the unbounded case is

$$\mathcal{G}_\Psi(\mathbf{x} - \mathbf{x}') = \frac{(RR')^{1/2}}{2\pi k R_0^2} [(2 - k^2) K(k^2) - 2E(k^2)] \tag{14}$$

where

$$k^2 = \frac{4RR'}{[(R+R')^2 + (Z-Z')^2]}$$

and $K(k^2)$ and $E(k^2)$ are the usual elliptic integrals. For bounded flows, an appropriate image vorticity contribution should be added to the Green function. Once the Green function is defined, the stream function $\Psi(\mathbf{x})$ for any source distribution $\Omega(\mathbf{x})$ can be obtained as

$$\Psi(\mathbf{x}) = \int \mathcal{G}_\Psi(\mathbf{x} - \mathbf{x}') \Omega(\mathbf{x}') d\mathbf{x}'$$

and thus the energy W (or the Hamiltonian) can be written as

$$W = \frac{1}{2} \int \Omega(\mathbf{x}) d\mathbf{x} \int \mathcal{G}_\Psi(\mathbf{x} - \mathbf{x}') \Omega(\mathbf{x}') d\mathbf{x}'.$$

The fluid flow energy is thus a quadratic function of the microscopic vorticity field $\Omega(\mathbf{x})$. To express this in terms of the macroscopic or average vorticity $\overline{\Omega}$, we first define a macroscopic stream function $\overline{\Psi}(\mathbf{x})$ as

$$-\Delta^* \overline{\Psi} = R^2 \overline{\Omega} \tag{15}$$

and write the flow kinetic energy as

$$W = \frac{1}{2} \int_V \overline{\Psi}\, \overline{\Omega}\, dx. \tag{16}$$

There is a fundamental assumption involved in writing Eq. (16), using Eqs. (5) and (15). We have ignored the contribution to the total flow energy from microscopic vorticity fluctuations whereas that due to large scale flow is aptly captured. This assumption of separation of length scales allows us to write the total flow energy in terms of the mean vorticity and mean stream function. Physically, it amounts to having averaged out the smallest vorticity scales. Thus only the *mean field* is considered. We present more discussion of this assumption and its limitations toward the end of this paper (see Sec. V).

Now that all physical quantities such as Casimirs, fluid impulse, and flow energy are expressed in terms of the macrostate probability field $\{e_i(\mathbf{x})\}$, we proceed to obtain the most probable macrostate out of all possible states consistent with the conservation laws. For this purpose, the free energy $\mathcal{F}$ of the system may be defined as

$$\mathcal{F} = S - \beta W - \gamma P - \sum_{i=1}^{n-1} \mu_i A_i \tag{17}$$

where β, γ, and μ_i $(i = 1, \ldots, n-1)$ are undetermined Lagrange multipliers for the flow energy, fluid impulse, and Casimirs (which includes circulation as its simplest case) while S, W, P, and A_i are defined through Eqs. (9), (16), (12), and (10), respectively. Note that, since the local probability $\Sigma_{i=1}^n e_i(\mathbf{x}) = 1$ is conserved, one of the unknowns can be eliminated. Upon extremizing the free energy functional with respect to arbitrary δe_i variations subject to $\Sigma_{i=1}^n e_i(\mathbf{x}) = 1$, we obtain, after some straightforward calculation, the most probable probability distribution for various vorticity levels, $\{e_i^*\}$, as

$$e_i^* = \frac{1}{\{1 + \Sigma_{i=1}^{n-1} \exp[\mu_i + a_i \beta \overline{\Psi} + a_i \gamma (R^2 - R_0^2)]\}}. \tag{18}$$

Here we have set $\mu_n \equiv 0$ without loss of generality. The asterisk indicates that the state is an extremum free energy state. With this expression for the most probable probability distribution function, we may express the complete set of equations for bounded axisymmetric Euler flows and the so-called rugged constants of motions in terms of the *averaged* macroscopic quantities as follows:

$$\overline{\Omega}^*(\mathbf{x})=\sum_{i=1}^{n} a_i e_i^*(\mathbf{x}),$$

$$-\Delta^*\overline{\Psi}^*=R^2\overline{\Omega}^*,$$

$$W(\Omega^0(\mathbf{x}))=\frac{1}{2}\int_V \overline{\Omega}^*\overline{\Psi}^* d\mathbf{x},$$

$$P(\Omega^0(\mathbf{x}))=\frac{1}{2}\int_V \overline{\Omega}^*(R^2-R_0^2)d\mathbf{x}, \qquad (19)$$

$$C(\Omega^0(\mathbf{x}))=\int_V \overline{\Omega}^* d\mathbf{x},$$

with

$$\overline{\Psi}(R=R_1,Z)=\overline{\Psi}(R=R_2,Z)=0,$$

$$\overline{\Psi}(R,Z=Z_1)=\overline{\Psi}(R,Z=Z_1).$$

$e_i^*(\mathbf{x})$ is given by Eq. (18); $R=R_1$, $R=R_2$, $Z=Z_1$, and $Z=Z_2$ are the confining boundaries (see Fig. 1) and are defined by $R_2-R_1=2b$, $R_2+R_1=2R_0$, $Z_1=-b$, and $Z_2=b$; R_0 is the mean distance between R_1 and R_2. (Here the boundary conditions on $\overline{\Psi}$ are formal. Our results do not depend on them. Thus, one could use *no-slip* conditions as well.)

For a given initial vorticity field $[\Omega^0(\mathbf{x})]$ (which in turn would completely fix the values of $[W,P,C]$) and boundary conditions, Eq. (19) gives the statistical mechanical description of the system at $t=\infty$. Note that, in general, the equations are nonlinear, with nonlinear integral constraints (nonlocal) and hence may involve multiple solutions and bifurcations. Also, in cases of physical interest like coherent structures, β is generally negative. This can be seen as follows. The inverse temperature β is defined as $\beta=\partial S/\partial W$, which is the ratio of the change in entropy of a system to a given change in total energy. If β is negative, then it implies that for an *increase* in the energy, the entropy of the system *decreases* or the system goes to a more *organized* state and hence coherent structures. Therefore, in the statistical theory of turbulence, $\beta<0$ necessarily implies merger of vortices or formation of coherent structures. In the next section, we solve these equations for a simple case and show that indeed they are rich and complex solutions to the stated problem. For convenience, in what follows, the asterisk will be dropped from the macroscopic variables.

IV. NUMERICAL RESULTS: THE CASE OF TWO VORTICITY LEVELS

As an example, we consider initial conditions with only two vorticity levels, viz., 0 and a (say). Even in this simple case, we do not know any way of solving the problem analytically. Hence in this section we compute numerical solutions for the two-level case.

In solving Eq. (19), we use the following scaling: the distances are scaled to b (half the length between two walls along $\hat{R}$), the vorticity is scaled to a, its maximum value, and the stream function is scaled to circulation C $(\equiv b^3a)$. Consequently, the velocity is scaled to C/b^2, the energy to C^2, the fluid impulse to Cb^2, β to b^3/C, and γ to b/C. Hence, the maximum vorticity level a becomes equal to 1. [Note that a has the dimensions of vorticity/length; hence C_0 has the correct dimensions of vorticity×(length)^2.] In the following sections, we use the same variables as before, but it is to be understood that they are in dimensionless form. Thus the boundaries extend from $R_1=1/\epsilon-1$ to $R_2=1/\epsilon+1$ along $\hat{R}$ and from -1 to 1 along $\hat{Z}$, where ϵ is the inverse aspect ratio defined as $\epsilon=b/R_0$, which is bounded by $0<\epsilon<1$.

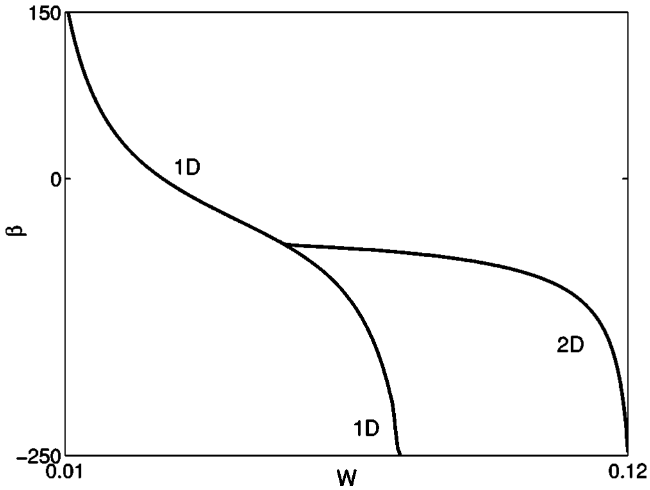

FIG. 2. β-W curve using the TW algorithm. Bifurcation from 1D to 2D is also shown.

Solutions to Eq. (19) are constructed using a scheme due to Turkington and Whitaker [30] (TW) for a given value of the set (W,C,P). The TW algorithm, which is an efficient scheme for constructing solutions of Eq. (19) when there are multiple solutions, relies on the fact that in the negative temperature regime the entropy density is a concave functional while the energy density is a convex function of $e_a(\mathbf{x})$. As a result the iteration procedure quickly converges to the solution with the desired number of vortices from an initial guess seeded with the same number of vortices. In our numerical procedure, the solution $\overline{\Psi}$ in each subiteration converges with a relative accuracy of $(1–5)\times10^{-7}$. The variational problem is considered solved if the (maximum) relative error between two successive iterations for $e_a(\mathbf{x})$ and W is of the order $(1–5)\times10^{-3}$. The initial seed is so chosen that it conserves the circulation constraints C and P and has seed energy $W_0>W$. Typically, for a given set (W, C, P), the TW scheme takes 10–15 iterations.

We show typical phase diagrams in Figs. 2–4, calculated using the TW algorithm with $C=2$ and $P=1.361$. For the rest of the calculations ϵ is set equal to 0.9 unless stated otherwise. Physically, specifying a value for ϵ amounts to fixing the distance from the geometric center of the bounded region to the $\hat{Z}$ axis (see Fig. 1). At the outset, one can see from Fig. 2 that the energy is bounded from above and be-

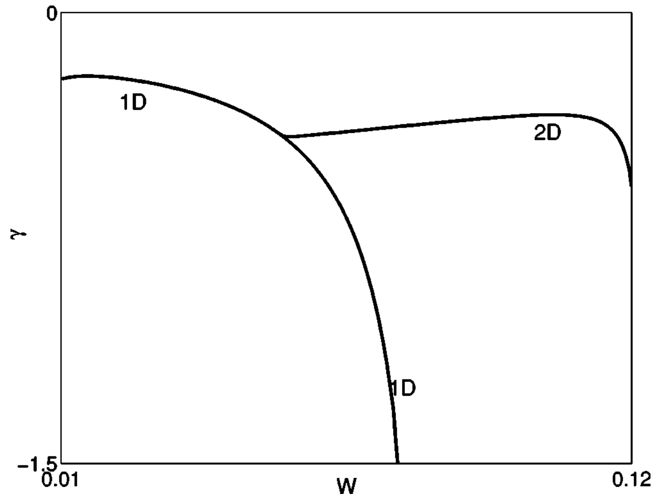

FIG. 3. γ-W curve using the TW algorithm. Bifurcation from 1D to 2D is also shown. Note that there are multiple energy values for a given γ in some regions.

low, implying that there are a minimum and a maximum of the energy at which the inverse temperature β is positive and negative, respectively. Now, note that the phase curve for β vs W shows three distinct regimes. (i) At low energies, there is a positive β region (see Figs. 2 and 4), where with increase in energy the entropy of the system increases, implying $\beta = \partial S/\partial W > 0$; (ii) at a particular energy value (say W_c), the entropy reaches a maximum value and β goes to 0; (iii) after W_c, with increase in energy β goes to negative values. With further increase in energy, there is the onset of a bifurcation phenomenon which leads to 1D and 2D solutions; in this region, there is a steep increase in the values of β. In the negative β regime, note that the entropy of the system decreases with increase in energy. In the $\beta > 0$ regime, as the entropy increases with increasing energy, these 1D states are diffuse (or unconfined) in nature, with more $\overline{\Omega}$ distribution toward the boundaries than in the center; $\beta \simeq 0$ implies a

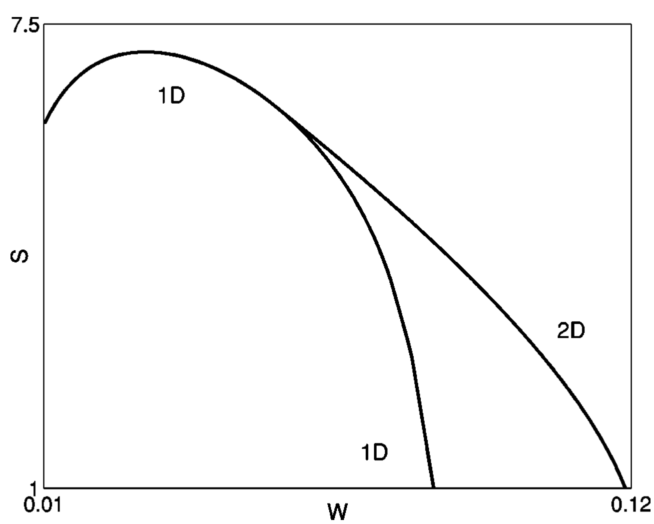

FIG. 4. S-W curve. Note that the entropy of the 1D solution is smaller and that of the 2D solution is large at a chosen value of energy after bifurcation.

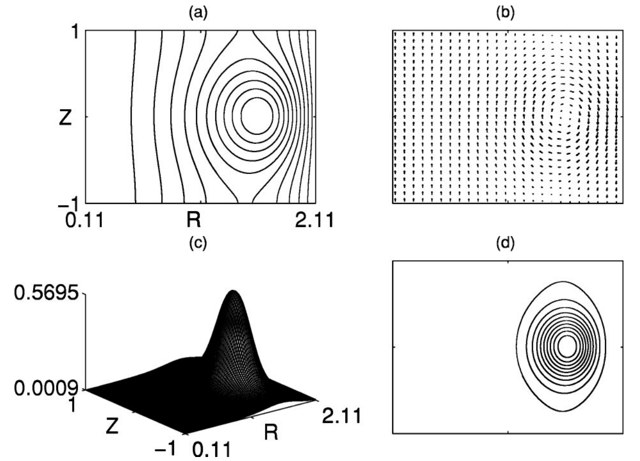

FIG. 5. Equilibrium solutions for $C=2$, $P=1.361$, and $W=0.07$. (a) shows equi-$\overline{\Psi}$ contours; (b) shows the corresponding flow profile—note that the flow is finite at the R boundaries; (c) shows the surface plot of $\overline{\Omega}$ exhibiting the nonuniform nature of the "fat ring;" (d) is a contour plot of (c). For presentation purposes, the labels in (b) and (d) are suppressed; they are the same as in (a).

nearly homogeneous $\overline{\Omega}$ distribution, which would be expected in an infinite temperature system. Our interest will be primarily in the region of formation of 2D coherent structures with both nonuniform and uniform distributions of $\overline{\Omega}$. Thus we will concentrate on the bifurcated 2D domain with energies $W > W_c$, where W_c is the energy where $\beta = 0$. Studies regarding bifurcation in the ring configuration have been extensive [31,32]. In the following sections, we will concentrate only on the negative β regime.

A. Finite negative β regime: Nonuniform vortex rings

As discussed before, negative β implies coherent (or confined) equilibria with peaked $\overline{\Omega}$ distributions. To clearly bring out the basic feature(s) of this model, we present in Figs. 5 and 6 solutions at two distinct values of $-\beta$ or W. Note that the larger the value of negative β (or W), the more coherent are the solutions and the smaller is the corresponding entropy. In the past, the concept of the ordering of entropy of negative temperature states has served as a model for "explaining" coherent structure formation in 2D large Reynolds number turbulence in both screened and unscreened systems [32,36].

For energies in the intermediate range where the corresponding β values are negative but finite (Fig. 5), the coherent vortex ring has a nonuniform distribution. The mean position of this "fat ring" along $\hat{R}$ is defined by the value of P while the extent of the nonzero region of distribution depends on the total circulation, as the peak vorticity a is scaled to unity. Since the boundary conditions are periodic, the $\overline{\Omega}$ peak, in principle, could be positioned anywhere along $\hat{Z}$. One could choose $Z=0$ as the mean peak position by appropriate choice of the initial condition in the TW algorithm.

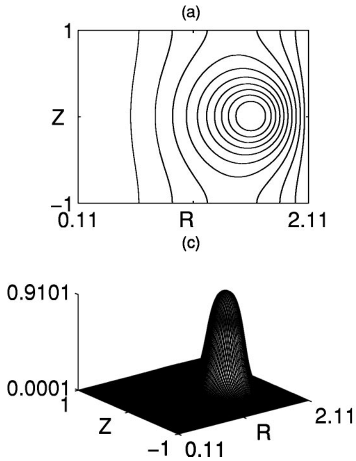

FIG. 6. Equilibrium solutions for $C=2$, $P=1.361$, and $W=0.10$ with the same meaning as in Fig. 5. For given values of C and P, as the energy W increases the profiles tend to become more coherent. For presentation purposes, the labels in (c) and (d) are suppressed; they are the same as in (a).

Since the impulse constraint is geometric in nature and the system is bounded in $\hat{R}$ (note that the boundary condition along $\hat{R}$ is free slip), there will be bounds on the allowed values of P for a given value of ϵ. Since the energy W and impulse P are independent isolating integrals, following Ref. [32], we set $\beta=0$ [such that Eq. (19) becomes linear in $\overline{\Psi}$] and obtain $P=P(\epsilon,\gamma_1)$ (which in turn can be solved for bounds on P) as

$$P=\frac{C}{2}\left[1+\frac{1}{\gamma_1}-\frac{2}{\epsilon}\coth\left(\frac{2\gamma_1}{\epsilon}\right)\right]. \tag{20}$$

Note that for a given value of ϵ, the absolute of P, i.e., $|P|$, is bounded (say $P_{\max}$) as a function of γ_1; as $\epsilon\to 0$, this bound not only increases in magnitude, but also becomes symmetric with respect to the $P=0$ line. Similarly, as $\epsilon\to 1$, the bound becomes asymmetric with respect to $P=0$ while the magnitudes are small but finite. These features are brought out in Fig. 7, where we have shown how the profile of $P/P_{\max}$ changes with ϵ. As described in Ref. [32], although Eq. (20) was obtained for $\beta=0$, due to the geometric nature of the constraint, the bounds thus obtained remain valid for any nonzero value of β.

Next, to bring out the effect of the P constraint on the $\overline{\Omega}$ distribution, we show in Fig. 8 the $\overline{\Omega}$ contours at the same values of energy and circulation, but for two different values of P (of course, well within the bounds). Clearly, the P values affect the mean position of the fat ring; that is, the radial position of the fat ring is essentially governed by the value of P. Thus, at any finite negative β value, the distribution of $\overline{\Omega}$ is nonuniform. Moreover, the speed of the fat ring, γ (W of Norbury's work [16,17]), and its shape emerge naturally out of our problem, once P and W are specified.

As we show in the next section, although our model is *statistical* in nature, when the vorticity fluctuations are small, i.e., when $\beta\to-\infty$ (i.e., wherever the vorticity is nonzero),

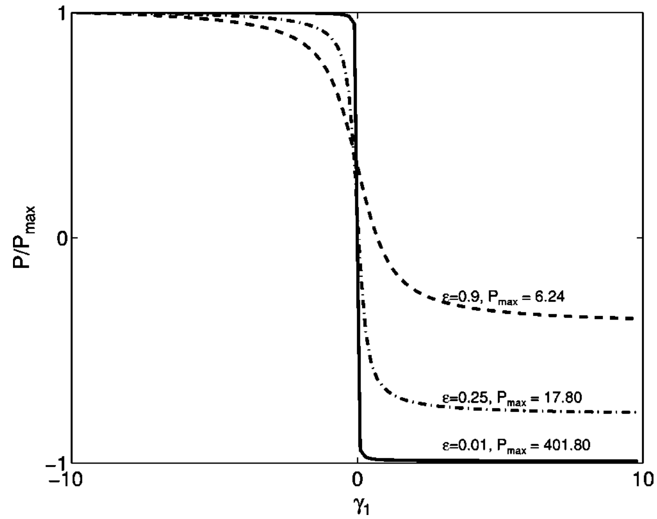

FIG. 7. Plot of Eq. (20) for various values of ϵ. As $\epsilon\to 1$, the asymmetry about $P=0$ increases whereas $P_{\max}$ itself decreases.

$e_a(\mathbf{x})$ becomes nearly equal to 1, and zero otherwise. Consequently, one may obtain a *deterministic* model for bounded domains as a limiting case, similar to those obtained in Refs. [15–17] for unbounded domains.

B. Infinite negative β regime: Uniform vortex rings

It is worthwhile to note that, unlike the point vortex formulation, which has no energy bounds (as two vortex rings of zero size can come arbitrarily close to each other) and hence has no zero entropy solutions (Kraichnan collapse sets in), a hard core vortex ring model (such as ours) admits zero entropy solutions, in the limit $\beta\to-\infty$. As noted by earlier

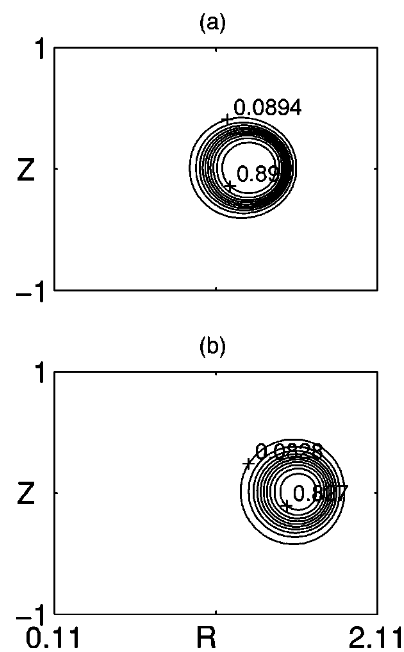

FIG. 8. Contours for two values of P, namely, $P=1.361$ and 2.045, for fixed values of W and C. As P increases, the mean position of the fat ring along R increases, and vice versa.

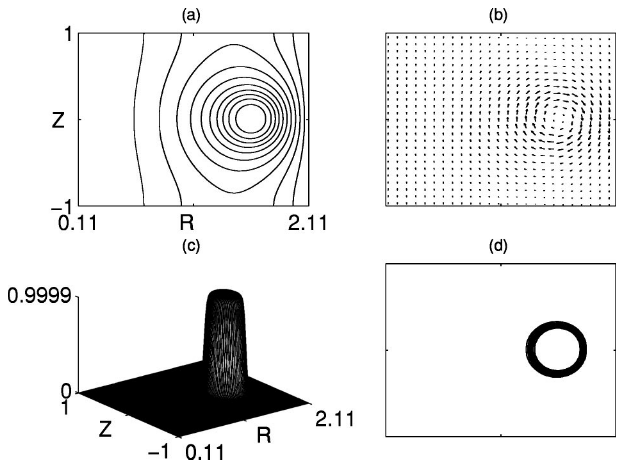

FIG. 9. Equilibrium solutions for given values of *C, P*, and *W* $=0.12$. Note that the solutions are nearly deterministic, meaning that $\overline{\Omega}$ is nearly uniform on the fat ring and falls off sharply at the edge. Note that the entropy $S\simeq 0.95$ as compared to its maximum value of $S\simeq 7.3$ at $\beta=0$. For presentation purposes, the labels in (b) and (d) are suppressed; they are the same as in (a).

workers for planar flows [29,30], within such a statistical model, as $\beta\to-\infty, e_a\to 1$, implying that the deterministic limit is embedded as the zero entropy solution in our statistical theory. Hence, one might expect that, for a given ϵ value, the limit $\beta\to-\infty$ would yield the deterministic solution for these boundary conditions. In Fig. 9, we show a (nearly) deterministic solution obtained for large $-\beta$. Clearly, $\overline{\Omega}$ is *nearly uniform* across the fat ring and falls off sharply to zero, mimicking a deterministic solution. To make this point clear, let us rewrite β as $\beta=-1/|T|$ such that the expression for the free energy [Eq. (17)] for the two-level case becomes

$$\tilde{F}=|T|S+W-\tilde{\gamma}P-\tilde{\mu}C \tag{21}$$

where $|T|$ is the absolute temperature. (Note that, as the area A_i occupied by the vorticity level a and the circulation C differ only by a constant a, which may be absorbed in $\tilde{\mu}$, we have replaced A_i by C.) According to our model, as $|T|\to\infty$, $S\to 0$ such that $|T|S\to\alpha$, where α is some constant. Since the total energy is only the flow energy (which includes fluctuating flow plus steady flow), in the limit where the entropy goes to zero (i.e., the large energy limit), the total energy is due only to the steady flow, which is already contained in W. Thus α becomes zero. In general, one may redefine W as $W+\alpha=\tilde{W}$ irrespective of the value of α. Thus Eq. (21) becomes

$$\tilde{F}=\tilde{W}-\tilde{\gamma}P-\tilde{\mu}C. \tag{22}$$

Hence extremization of the free energy in the limit $\beta\to-\infty$ amounts to extremization of the energy subject to the constraints of P and C. Wan [20] has already shown that Hill's spherical vortex is the maximum energy state subject to the P constraint and Norbury's class of vortices are the maximum energy state subject to both P and C constraints. Thus our model could be viewed as the generalization of Wan's results to bounded systems with appropriate boundary conditions in the limit when $\beta\to-\infty$. Of particular interest would be the limit $\epsilon\to 1$, $\beta\to-\infty$, $P\to-P_{\max}$ for any arbitrary C, which would be the equivalent of Hill's spherical vortex in the current context.

V. DISCUSSION

As mentioned before, our model is based on the works of Miller *et al.* [10] and Robert and Sommeria [11] for planar Euler flows. Therefore, we discuss here the core issues, which are relevant to both planar and axisymmetric flows.

As is common to many other physical models that construct a thermal equilibrium measure, the unproven assumption of *ergodicity* is at the heart of the present work. Although it is well known that a collection of "point vortices" $(N>3)$ in a 2D planar flow is chaotic [37] and may well be mixing, it is not clear if for any given initial condition the continuum dynamics will eventually be ergodic. There are many examples of initial conditions that are mixing as well as the nonmixing kind. Thus, the justification for our assumption of ergodicity should come *a posteriori*. However, it should be mentioned here that, if not ergodicity, it was shown by Robert and Sommeria [11] that a concentration property does exist [that is, a great majority of microscopic vorticity fluctuations (microstates) $\Omega(\mathbf{x})$ are concentrated around a macrostate $\{e_i(\mathbf{x})\}$]. Therefore, if ergodicity is indeed satisfied, then at infinite time the flow will most probably stay near this macrostate.

The second crucial issue common to planar and axisymmetric flows discussed here is the assumption of scale separation: meaning that, while the microscopic vorticity fluctuations contribute to the entropy functional, the very same fluctuations are completely ignored while computing the total flow energy of the system. In other words, the microscopic fluctuations are averaged out and only the mean flow contribution to the total energy is considered. Such a separation of vorticity scales allows one to attain closure. Thus, whereas this class of statistical model may well capture the large scale features, the results may not in general be true. Recently, Chorin [33] presented some numerical evidence for the case of three-level [i.e., $(0,1,-1)$] vorticity, in which the MR statistics is shown to be invalid for large energies (large negative β values), whereas reasonable agreement is shown at low or intermediate energy ranges.

In spite of these outstanding issues, the problem of formulation of statistical equilibrium theories for planar and axisymmetric flows is interesting for the following reasons. There has been numerical evidence showing the emergence of coherent structures from (nearly) arbitrary initial conditions in the case of incompressible, inviscid, large Reynolds number 2D turbulence [1]. Furthermore, the numerical simulations reported in Ref. [12] for an annulus are encouraging. Finally, there have been a number of useful qualitative as well as quantitative predictions based on these models. For example, the results of experiments in non-neutral electron plasmas trapped in an applied magnetic field [35] agree well with the predictions of these statistical models. So do the numerical experiments on Euler and quasigeostrophic flows [34]. From these considerations, we take the standpoint that it is still premature to conclude anything from the negative results obtained hitherto for planar Euler flows.

In the present work, we have developed a statistical mechanical model for an incompressible, inviscid, axisymmetric Euler flow. Due to the nature of the governing equations, the vorticity per unit length (which we have called the vorticity throughout) is conserved by the flow dynamics. Thus the role of vorticity in planar Euler flows is assumed by $\Omega \equiv \omega/R$ in axisymmetric flows. Once cast in the form of a transport equation for Ω, the axisymmetric and planar flows fall into the same class of noncanonical Hamiltonian flows.

The late time states are defined completely by specifying the initial vorticity field, which in turn specifies the values of constants of motion. To illustrate various features of our model, we have numerically solved the equations for the case of two-level vorticity. In particular, we show that finite size vortex rings are convex when they are typically characterized by negative β values. Thus, nonuniform vortex rings are obtained when β is negative and finite while uniform vortex rings result for infinite negative β. In the latter limit, we argue that, due to the absence of vorticity fluctuations (the entropy goes to zero), this class of solutions may be considered as ''deterministic.'' This then could be the bounded analog of the past work of Wan [20] and Norbury [16,17]. Moreover, in contrast to the past work, here, specifying the values of global constraints, namely, *W,C,P*, completely determines the shape and speed of the vortex and the position of the vortex center with respect to the axis.

[1] J. C. McWilliams, J. Fluid Mech. **219**, 361 (1990).
[2] L. Onsager, Nuovo Cimento, Suppl. **6**, 279 (1949).
[3] J. B. Taylor, Phys. Lett. **40A**, 1 (1972).
[4] D. Montgomery and G. Joyce, Phys. Fluids **17**, 1139 (1974).
[5] S. F. Edwards and J. B. Taylor, Proc. R. Soc. London, Ser. A **336**, 257 (1974).
[6] J. C. E. Seyler, Jr., Phys. Rev. Lett. **22**, 515 (1974); Phys. Fluids **19**, 1336 (1976).
[7] Y. B. Pointin and T. S. Lundgren, Phys. Fluids **19**, 1459 (1976); T. S. Lundgren and Y. B. Pointin, Phys. Fluids **20**, 356 (1977).
[8] R. H. Kraichnan and D. Montgomery, Rep. Prog. Phys. **43**, 547 (1980).
[9] V. L. Berdichevsky, Phys. Rev. E **52**, 4432 (1995).
[10] J. Miller, Phys. Rev. Lett. **65**, 2137 (1990); J. Miller, M. C. Cross, and P. B. Weizmann, Phys. Rev. A **45**, 2328 (1992).
[11] R. Robert and J. Sommeria, J. Fluid Mech. **229**, 291 (1991).
[12] P. C. Marcus, Nature (London) **331**, 693 (1988).
[13] A. Thess, J. Sommeria, and B. Juttner, Phys. Fluids **6**, 2417 (1994).
[14] K. Maruhn, Math. Z. **39**, 244 (1934).
[15] L. E. Fraenkel, Proc. R. Soc. London, Ser. A **316**, 29 (1970).
[16] J. Norbury, J. Fluid Mech. **72**, 253 (1972).
[17] J. Norbury, J. Fluid Mech. **57**, 417 (1973).
[18] H. Lamb, *Hydrodynamics* (Cambridge University Press, Cambridge, England, 1932).
[19] L. E. Fraenkel, J. Fluid Mech. **51**, 119 (1972).
[20] Y. H. Wan, Trans. Am. Math. Soc. **308**, 299 (1988).
[21] S. E. Widnall and J. P. Sullivan, Proc. R. Soc. London, Ser. A **332**, 335 (1973).
[22] S. E. Widnall and C.-Y. Tsai, Philos. Trans. R. Soc. London, Ser. A **287**, 273 (1977).
[23] K. Shariff and A. Leonard, Annu. Rev. Fluid Mech. **24**, 235 (1992).
[24] M. Gharib, E. Rambod, and K. Shariff, J. Fluid Mech. **360**, 121 (1998).
[25] P. G. Saffman, *Vortex Dynamics*, Cambridge Monographs on Mechanics and Applied Mathematics (Cambridge University Press, Cambridge, England, 1995), Chaps. 3 and 10.
[26] J. E. Marsden and A. Weinstein, Physica D **7**, 305 (1983).
[27] P. J. Olver, *Applications of Lie Groups to Differential Equations* (Springer-Verlag, New York, 1986).
[28] D. Holm, J. E. Marsden, T. Ratiu, and A. Weinstein, Phys. Rep. **123**, C1 (1985).
[29] N. Whitaker and B. Turkington, Phys. Fluids **6**, 3963 (1994).
[30] B. Turkington and N. Whitaker, SIAM J. Sci. Comput. (USA) **6** (12), 3963 (1996).
[31] R. Ganesh, Ph.D. dissertation, Institute for Plasma Research, Bhat, Gandhinagar, India, 1998.
[32] R. Ganesh and K. Avinash, Phys. Lett. A **265**, 97 (2000).
[33] A. J. Chorin, Phys. Fluids **8**, 2656 (1996).
[34] J. Sommeria, C. Staquet, and R. Robert, J. Fluid Mech. **233**, 661 (1991); J. Michel and R. Robert, J. Stat. Phys. **77**, 645 (1994).
[35] D. H. E. Dubin and T. M. O'Neil, Rev. Mod. Phys. **71**, 87 (1999).
[36] R. Ganesh and K. Avinash, Phys. Plasmas **7**, 3947 (2000).
[37] H. Aref, Annu. Rev. Fluid Mech. **15**, 345 (1983).